Herding CATs: A Comparison of Linear Chromatic-Adaptation Transforms for CIECAM97s

Anthony J. Calabria and Mark D. Fairchild
Munsell Color Science Laboratory, Rochester Institute of Technology
Rochester, NY

Abstract

There are currently five transformation matrices being considered for use in the linear chromatic-adaptation transform in a revision of the CIECAM97s color appearance model. Four of the matrices were developed independently for the purpose of transforming tristimulus values to spectrally sharpened RGB responses. The fifth is the Hunt-Pointer-Estevez transform of CIE tristimulus values to normalized cone responsivities. RGB images were transformed between CIE illuminant D65 and CIE illuminant A white point using each of the matrices and results were examined visually. In addition, pixel-wise ΔE^*_{94} and ΔE^*_{ab} calculations between corresponding color images showed the performance of the four XYZ-to-RGB transformation matrices was essentially equal. In a complex image, these slight differences would most likely go undetected.

Introduction

Color appearance models are tools used to predict perceived changes in a color based on changes in environmental factors. Color appearance models are extensions of traditional colorimetry in that they incorporate factors such as change of illuminant, surround, and degree of adaptation to the source. A chromatic-adaptation transform (CAT) is used to predict corresponding colors by comparing appearance under two different illuminants (for example, D65 and A). The CIE 1997 Interim Color Appearance Model (Simple Version), abbreviated CIECAM97s, was proposed by CIE TC1-34 in 1997 in response to the needs of the imaging industry for a single, practically-applicable color appearance model for device-independent color imaging applications[1]. The color appearance model includes a modified von Kries type chromatic-adaptation transform employing an XYZ-to-RGB transformation matrix for conversion from normalized tristimulus values to spectrally sharpened cone responses. The CIECAM97s CAT equations currently include an exponential function for adaptation in the short wavelength channel. This nonlinearity forces the normalization of tristimulus values to the Y values of the stimulus and renders CIECAM97s uninvertible[1]. CIECAM97s in this form was recommended as an interim solution for practical applications requiring more sophistication than that offered by CIELAB.

Modifications to CIECAM97s have since been proposed by Fairchild[1] including the linearization of the chromatic-adaptation transform to simplify the model and facilitate inversion. The incorporation of a linear CAT required the development of a new XYZ-to-RGB transform. A transformation matrix for the linear CAT was proposed by Fairchild. The Fairchild matrix (Equation 1) was derived by optimization of corresponding colors of real samples

$$M_{Fairchild} = \begin{bmatrix} 0.8562 & 0.3372 & -0.1934 \\ -0.8360 & 1.8327 & 0.0033 \\ 0.0357 & -0.0469 & 1.0112 \end{bmatrix} \quad (1)$$

from the *Munsell Book of Color* in order to minimize change from the original CIECAM97s predictions. Susstrunk et al.[2] have proposed a preliminary matrix (Equation 2) based on white point preserving data-based

$$M_{Susstrunk} = \begin{bmatrix} 1.2694 & -0.0988 & -0.1706 \\ -0.8364 & 1.8006 & 0.0357 \\ 0.0297 & -0.0315 & 1.0018 \end{bmatrix} \quad (2)$$

sharpening of the Lam corresponding color data set. A matrix was proposed by Li et al.[3] (Equation 3) optimized for minimum mean ΔE^*_{ab} of 11 experimental data sets. The

$$M_{Li\ et\ al} = \begin{bmatrix} 0.7982 & 0.3389 & -0.1371 \\ -0.5918 & 1.5512 & 0.0357 \\ 0.0008 & 0.0239 & 0.9753 \end{bmatrix} \quad (3)$$

cone responses for the Li et al. matrix are sharper than those of the original CIECAM97s color appearance model. A modified version of Li et al. has also been proposed (Equation 4). The fifth transform matrix which could be

$$M_{\text{mod Li et al}} = \begin{bmatrix} 0.7328 & 0.4296 & -0.1624 \\ -0.7036 & 1.6974 & 0.0061 \\ 0.0030 & 0.0136 & 0.9834 \end{bmatrix} \quad (4)$$

considered for use in the linear CAT is the Hunt-Pointer-Estevez cone responsivities matrix (Equation 5). Interesting to note, the Hunt-Pointer-Estevez matrix is used later in CIECAM97s to transform the sharpened cone sensitivities to normal cone responsivities prior to the application of a nonlinear response compression.

$$M_{\text{Hunt et al}} = \begin{bmatrix} 0.38971 & 0.68898 & -0.07868 \\ -0.22981 & 1.18340 & 0.04641 \\ 0.00 & 0.00 & 1.00 \end{bmatrix} \quad (5)$$

Figures 1-3 illustrate the similarities of tristimulus weights for the RGB channels used by the five matrices. Since the matrices were developed for the same purpose, similarities were expected. Although the transformations have the same likenesses, significant differences can be observed in the red and green channel weights.

The chromatic-adaptation transform is a von Kries type transformation to model human correction for the color of the illuminant. As mentioned above, the nonlinearity from the original proposal of CIECAM97s has been removed.

$$R_c = \left[D(100/R_w) + 1 - D\right]R \quad (6)$$

$$G_c = \left[D(100/G_w) + 1 - D\right]G \quad (7)$$

$$B_c = \left[D(100/B_w) + 1 - D\right]B \quad (8)$$

The spectrally sharpened cone responses for the stimulus (R,G,B) and illuminant white point (R_w,G_w,B_w) are used in Equations (6-8) to generate cone responses from a stimulus under equal-energy illumination (R_c,G_c,B_c) where D represents the level of adaptation (D=1 for complete adaptation in this case).

A pixel-wise comparison of corresponding image colors from each of the above transformation matrices is used as a tool to evaluate how extensively the matrices should be tested before possible incorporation in CIECAM97s. It was anticipated that the Hunt-Pointer-Estevez model will have the greatest difference from the other matrices because the Hunt et al. matrix was developed as a transform to cone responsivities rather than sharpened cone responses.

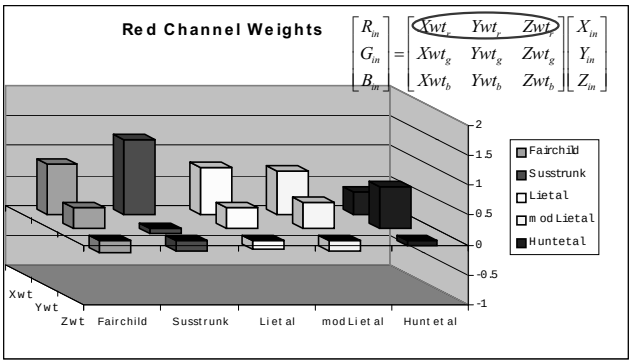

Figure 1. Red channel weights for each transformation matrix

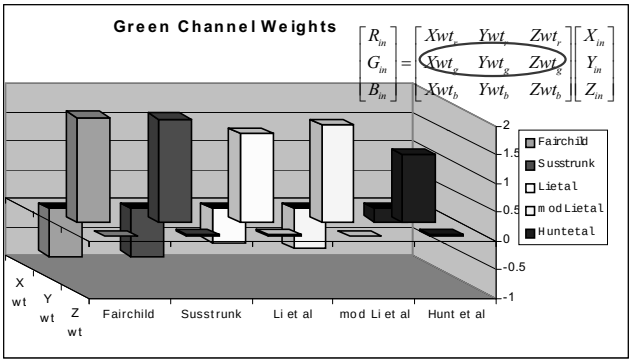

Figure 2. Green channel weights for each transformation matrix

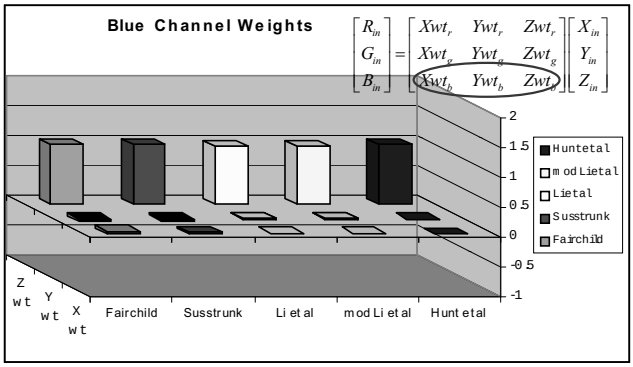

Figure 3. Blue channel weights for each transformation matrix

Experimental Procedure

Using the IDL 5.3 programming language on a Macintosh platform, a graphical user interface (GUI) program was developed to transform images between CIE illuminant D65 and CIE illuminant A white points. The GUI was designed for visualization of differences between images transformed by the five XYZ-to-RGB transforms proposed for use in the linear CAT for use in a revision of CIECAM97s.

Images were transformed between CIE illuminant D65 and CIE illuminant A white point by means of the linear CAT using each of the five transformation matrices separately. Corresponding color images were evaluated for mean ΔE^*_{94}, mean ΔE^*_{ab} between each of the corresponding color output images on a pixel-by-pixel basis (the output image of each XYZ-to-RGB transformation matrix is compared to the output images of the other four matrices). Images were output to the display for visual evaluation using an sRGB transform. The sRGB transform was chosen as a generic transform between XYZ and RGB for display. The goal of this program is to determine the spread of the data output by the CAT matrices. Therefore, since the outputs are color difference data calculated independently of output image display, this tool could properly calculate color differences between corresponding color images based on the five XYZ-to-RGB transforms for any input RGB image.

Chromatic-adaptation Transform Procedure—Upon reading an RGB image, the image RGB digital counts (subscripted with d for display) are normalized by 255 and transformed to normalized tristimulus values X_c, Y_c, Z_c by the inverse of the XYZ -to-sRGB matrix defined by Berns[4].

$$\begin{bmatrix} X_c \\ Y_c \\ Z_c \end{bmatrix} = \begin{bmatrix} 0.4124 & 0.3576 & 0.1805 \\ 0.2126 & 0.4751 & 0.0721 \\ 0.0193 & 0.1192 & 0.9505 \end{bmatrix} \begin{bmatrix} R_d \\ G_d \\ B_d \end{bmatrix} \quad (9)$$

Following a multiplication by input illuminant white point luminante (CIE illuminant D65 in this case, Equation 10), input tristimulus values are matrix multiplied by each of the five XYZ-to-RGB transformation matrices (represented as M_i in equation 11) generating five sets of spectrally-sharpened RGB cone responses (subscripted i representing each transformation matrix). Similar calculations to Equation (11) were performed for the white point

$$\begin{bmatrix} X \\ Y \\ Z \end{bmatrix} = \begin{bmatrix} X_c \\ Y_c \\ Z_c \end{bmatrix} * 100 \quad (10)$$

$$\begin{bmatrix} R_i \\ G_i \\ B_i \end{bmatrix} = M_i \begin{bmatrix} X \\ Y \\ Z \end{bmatrix} \quad (11)$$

tristimulus values of CIE illuminants D65 and A for later calculation. The input white point (CIE illuminant D65) RGB values are represented as Rw_i, Gw_i, Bw_i, while output illuminant (CIE illuminant A) white point RGB values are represented as $R'w_i$,$G'w_i$,$B'w_i$ in future equations. The transformed RGB values are then corrected through a modified von Kries type transform. Bearing in mind the scope of this project, adaptation is considered complete (D=1) and does not need to be considered in the chromatic-adaptation transform.

$$R_{ci} = \left[D(100/Rw_i) + 1 - D\right] R_i \quad (12)$$

$$G_{ci} = \left[D(100/Gw_i) + 1 - D\right] G_i \quad (13)$$

$$B_{ci} = \left[D(100/Bw_i) + 1 - D\right] B_i \quad (14)$$

At this point, the input RGB signals have been corrected for CIE illuminant D65 white point, and the process is inverted as tristimulus values under CIE illuminant A are desired. The post-adaptation signals are first transformed to spectrally-sharpened cone responses under CIE illuminant

$$\frac{R_{ci}}{D\left[(100/R'w_i) + 1 - D\right]} = R'_i \quad (15)$$

$$\frac{G_{ci}}{D\left[(100/G'w_i) + 1 - D\right]} = G'_i \quad (16)$$

$$\frac{B_{ci}}{D\left[(100/B'w_i) + 1 - D\right]} = B'_i \quad (17)$$

A. The spectrally-sharpened cone responses are transformed to CIE illuminant A tristimulus values by matrix multiplication with the inverse of the M_i matrix used in Equation (11).

$$\begin{bmatrix} X'_i \\ Y'_i \\ Z'_i \end{bmatrix} = M_i^{-1} \begin{bmatrix} R'_i \\ G'_i \\ B'_i \end{bmatrix} \quad (18)$$

Each of the five sets of tristimulus values is then transformed to CIELAB coordinates. Pixel-wise color differences were calculated between each set of corresponding color output images. Mean color differences and their associated standard deviations were examined.

Display Procedure—Images corresponding to the five possible transformation matrices were displayed in RGB. Tristimulus values were normalized by the white point luminance value and converted to normalized sRGB digital counts for display (Berns[4]).

$$\begin{bmatrix} R'_{di} \\ G'_{di} \\ B'_{di} \end{bmatrix} = \begin{bmatrix} 3.2410 & -1.5374 & 0.4986 \\ -0.9692 & 1.8760 & 0.0416 \\ 0.0556 & -0.2040 & 1.0570 \end{bmatrix} \begin{bmatrix} X'_i \\ Y'_i \\ Z'_i \end{bmatrix} \quad (19)$$

Normalized sRGB digital counts were then scaled by 255 for output on a 24-bit display. Images were output to

the screen within the GUI for visual assessment and comparison with the color difference data.

Results

Three example images were used to test the transformation matrices. One was an RGB image of a Macbeth Color Checker chart photographed under simulated CIE D65 illumination. The second was an RGB image consisting of eight colored spheres. This image was computer generated as an original under CIE D65 illumination conditions. The third image was a "rainbow gradient" generated in Adobe Photoshop. The *Rainbow Gradient* image was chosen because it consisted of high-chroma representations of the colors of the visible spectrum. This high-chroma image represents a worst-case scenario of what CIECAM97s could be used for. Although illumination conditions were not specified for the *Rainbow Gradient* image, it can be considered an independent test target of high chroma colors since color differences are calculated independent of display images.

Table 1. Mean color differences and standard deviations of corresponding color Macbeth Color Checker images.

Mean ΔE94 of *Macbeth Color Checker* Image					
CAT	Fairchild	Li et al	Mod Li et al	Susstrunk et al	Hunt et al
Fairchild		0.74	0.50	0.73	1.57
Li et al	0.75		0.35	0.93	1.16
Mod Li et al	0.50	0.35		0.89	1.40
Susstrunk et al	0.73	0.92	0.89		1.45
Hunt et al	1.55	1.13	1.37	1.43	
Standard Deviation ΔE94 of *Macbeth Color Checker* Image					
CAT	Fairchild	Li et al	Mod Li et al	Susstrunk et al	Hunt et al
Fairchild		0.81	0.54	0.90	1.82
Li et al	0.81		0.43	0.98	1.24
Mod Li et al	0.54	0.43		1.02	1.52
Susstrunk et al	0.89	0.97	1.01		1.77
Hunt et al	1.79	1.20	1.48	1.74	
Mean ΔEab of *Macbeth Color Checker* Image					
CAT	Fairchild	Li et al	Mod Li et al	Susstrunk et al	Hunt et al
Fairchild		1.38	1.02	1.19	2.62
Li et al	1.38		0.56	1.66	2.49
Mod Li et al	1.02	0.56		1.64	2.73
Susstrunk et al	1.19	1.66	1.64		2.53
Hunt et al	2.62	2.49	2.73	2.53	
Standard Deviation ΔEab of *Macbeth Color Checker* Image					
CAT	Fairchild	Li et al	Mod Li et al	Susstrunk et al	Hunt et al
Fairchild		1.77	1.41	1.48	3.26
Li et al	1.77		0.72	1.94	3.19
Mod Li et al	1.41	0.72		1.92	3.29
Susstrunk et al	1.48	1.94	1.92		3.28
Hunt et al	3.26	3.19	3.29	3.28	

Pixel-wise color difference calculations between corresponding color images of the *Macbeth Color Checker Chart* produced $\overline{\Delta E^*_{94}} < 0.93$, $\sigma_{94}{}^2 < 1.79$ and $\overline{\Delta E^*_{ab}} < 1.66$, $\sigma_{ab}{}^2 < 1.94$ for images transformed by the four matrices expected to produce similar results (Fairchild, Susstrunk et al., Li et al., Modified Li et al.). As expected, the image transformed by the Hunt et al. matrix resulted in higher color differences from the other transformed images.

Color difference calculations on the *Spheres* image resulted in $\overline{\Delta E^*_{94}} < 1.16$, $\sigma^2_{94} < 0.50$ and $\overline{\Delta E^*_{ab}} < 1.51$, $\sigma^2_{ab} < 0.91$ for images transformed by all five matrices. The small color differences between corresponding color images generated using the *Spheres* and *Color Checker* images are most likely undetectable in complex image comparison. Standard deviations indicate a tight distribution within the color difference data for both images and indicate the data produced by the different transformation matrices are reasonably close.

Table 2. Mean color differences and standard deviations of corresponding color Spheres images.

Mean ΔE94 of *Spheres* Image					
CAT	Fairchild	Li et al	Mod Li et al	Susstrunk et al	Hunt et al
Fairchild		0.49	0.49	0.86	0.55
Li et al	0.49		0.21	1.05	0.61
Mod Li et al	0.50	0.21		1.16	0.76
Susstrunk et al	0.86	1.05	1.16		0.75
Hunt et al	0.54	0.60	0.75	0.74	
Standard Deviation ΔE94 of *Spheres* Image					
CAT	Fairchild	Li et al	Mod Li et al	Susstrunk et al	Hunt et al
Fairchild		0.23	0.20	0.33	0.49
Li et al	0.24		0.10	0.43	0.40
Mod Li et al	0.21	0.10		0.50	0.45
Susstrunk et al	0.33	0.42	0.49		0.38
Hunt et al	0.48	0.38	0.43	0.38	
Mean ΔEab of *Spheres* Image					
CAT	Fairchild	Li et al	Mod Li et al	Susstrunk et al	Hunt et al
Fairchild		0.76	0.77	1.09	0.75
Li et al	0.76		0.24	1.38	0.92
Mod Li et al	0.77	0.24		1.51	1.08
Susstrunk et al	1.09	1.38	1.51		0.96
Hunt et al	0.75	0.92	1.08	0.96	
Standard Deviation ΔEab of *Spheres* Image					
CAT	Fairchild	Li et al	Mod Li et al	Susstrunk et al	Hunt et al
Fairchild		0.70	0.64	0.56	0.72
Li et al	0.70		0.14	0.88	0.96
Mod Li et al	0.64	0.14		0.91	0.97
Susstrunk et al	0.56	0.88	0.91		0.62
Hunt et al	0.72	0.96	0.97	0.62	

The *Rainbow Gradient* image was transformed both from a D65 to A white point as done above, as well as from A to D65 white points. As seen in Table 3, color differences and standard deviations of the high chroma *Rainbow Gradient* images are much greater than those of the *Color Checker* or *Spheres* images (Tables 1-2). The greatest differences occurred when transforming from CIE illuminant A to D65. Visual examination indicates high color differences may be due to hue shifts in blue regions of the image.

Table 3. Mean color differences and standard deviations of (D65-A) corresponding color Rainbow Gradient images.

Rainbow Gradient DE94					
D65-A	Fairchild	Li et al	mod Li et al	Susstrunk et al	Hunt et al
Fairchild		3.96	2.28	4.34	5.92
Li et al	4.01		2.06	3.69	3.47
mod Li et al	2.33	2.07		4.47	5.20
Susstrunk et al	4.36	3.64	4.43		4.33
Hunt et al	5.82	3.38	5.10	4.24	
Rainbow Gradient Stdev DE94					
D65-A	Fairchild	Li et al	mod Li et al	Susstrunk et al	Hunt et al
Fairchild		3.62	1.30	3.46	6.36
Li et al	3.53		2.33	1.53	2.16
mod Li et al	1.32	2.36		2.18	4.49
Susstrunk et al	3.42	1.47	2.14		2.31
Hunt et al	6.18	2.13	4.39	2.21	

Table 4. Mean color differences and standard deviations of (A-D65) corresponding color Rainbow Gradient images.

Rainbow Gradient DE94					
A-D65	Fairchild	Li et al	mod Li et al	Susstrunk et al	Hunt et al
Fairchild		5.56	2.51	4.35	12.20
Li et al	5.56		3.20	2.81	7.31
mod Li et al	2.51	3.19		3.40	10.18
Susstrunk et al	4.32	2.76	3.34		9.25
Hunt et al	12.34	7.38	10.32	9.41	
Rainbow Gradient Stdev DE94					
D65-A	Fairchild	Li et al	mod Li et al	Susstrunk et al	Hunt et al
Fairchild		3.79	0.95	3.27	11.32
Li et al	3.82		3.00	0.71	7.15
mod Li et al	0.95	2.98		1.86	10.29
Susstrunk et al	3.30	0.65	1.85		7.43
Hunt et al	11.59	7.28	10.53	7.62	

In the case of the illuminant A to D65 transform, errors may be enhanced due to high chroma blue regions of an image supposedly captured under a source with very little blue energy, being transformed to a source of high blue energy.

Conclusion

A GUI program was developed in IDL 5.3 [B] to evaluate and visualize color differences achieved by comparing the five possible XYZ-to-RGB transformation matrices currently under consideration for implementation in the linear chromatic adaptation transform in a modification to the CIECAM97s color appearance model.

The mean color differences of corresponding color images transformed between CIE illuminant D65 and CIE illuminant A white points were used to determine the significance of differences produced by the matrices. RGB images of color rendered spheres with CIE illuminant D65 white point and the Macbeth Color Checker chart photographed under simulated CIE illuminant D65 transformed to CIE illuminant A white point illustrated color differences between images transformed by the proposed matrices most likely will not be visible when viewed in a complex image. Standard deviations indicate the corresponding color images produce a tight grouping of color differences. Mean color difference calculations on a high chroma "rainbow gradient" indicated color differences between images transformed by the proposed matrices can be seen in a worst-case scenario of simple, high-chroma images.

References

1. Fairchild, M.D. A Revision of CIECAM97s for Practical Applications. In press Color Research and Application.
2. Susstrunk, S. et al.. Chromatic-adaptation performance of different RGB sensors. Proceedings of SPIE/IS&T Electronic Imaging 2001. P 172-178.
3. Li, C. et al.. Simplification of the CMCCAT97. Scottsdale: Proceedings of IS&T/SID 8th Color Imaging Conference; 2000. P 56-60.
4. Berns, R.S. Billmeyer and Saltzman's principles of color technology. John Wiley & sons, inc. New York. P 222.

Biography

Anthony Calabria received his B.S. degree in Imaging Science from Rochester Institute of Technology in 2000. He is currently a second year student of the M.S. Color Science program at the Munsell Color Science Laboratory at RIT. His thesis will include the study of observer preference of image contrast.

[B] Cross platform source code is available at http://www.cis.rit.edu/~ajc1961/Appearance